

OPTIMIZATION OF LASER PROCESSES IN n^+ EMITTER FORMATION FOR c-Si SOLAR CELLS

A. Orpella¹, I. Martín¹, S. Blaque¹, C. Voz¹, I. Sánchez², M. Colina², C. Molpeceres², R. Alcubilla¹

¹ Departament d'Enginyeria Electrònica, Universitat Politècnica de Catalunya
C/ Jordi Girona 1-3, Mòdul C4, 08034 Barcelona, Spain. Pho.: +34 93 405 41 93
Fax: +34 93 401 67 56, e-mail: orpella@eel.upc.edu

² Centro Láser UPM, Universidad Politécnica de Madrid
Ctra de Valencia Km 7.3, 28031, Madrid, Spain. Pho.: +34 91 336 55 41
Fax: +34 91 331 69 06, e-mail: misanchezaniorte@gmail.com

ABSTRACT: Punctual phosphorus diffused emitters were achieved by laser patterning phosphorus doped a-SiC_x:H films deposited by PECVD as a doping source. Two different lasers at wavelengths of 1064 nm and 532 nm were used. Phosphorus diffusion was confirmed by Secondary Ion Mass Spectroscopy. We explored the effect of pulse energy and number of pulses per diffused point. The results show that a fine tune of the energy pulse is critical while the number of pulses has minor effects. Scanning Electron Microscopy (SEM) pictures and optical profilometry showed a laser affected area where the c-Si is melted, ejected and solidified quickly again. Typically, the diameter of the affected area for 1064 nm laser is between two and four times greater than for 532 nm laser. Optimum parameters for both lasers were determined to obtain best J-V curves nearly to ideal diode behavior. Comparing best J-V results, lower emitter saturation current density (J_0) and contact resistance are obtained with 532 nm laser. The improvement in J_0 can be related mainly to the smaller affected areas observed by SEM while lower contact resistance can be attributed to that 532 nm laser has a more superficial action resulting in higher phosphorus concentration at the surface. The expected open voltage circuit for finished solar cells using these emitters is in the range of 640 mV for 532 nm laser and 620 mV for 1064 nm one.

Keywords: c-Si, diffusion, laser processing, a-SiC_x:H

1. INTRODUCTION

In most industrial solar cells based on c-Si substrates, the n^+ -p junction is created by diffusion of phosphorus atoms in a conventional furnace. This classical process typically needs temperatures of about 800-900 °C for several minutes becoming one of the most expensive and time-consuming processes in the fabrication line. Recently, the introduction of laser processing in these devices opens an alternative to the conventional diffusion. A first approach is the n^+ emitter formation along the entire cell area by scanning it with a focused laser beam and using a spin-on dopant as a doping source [1-2]. Moreover, the formation of any desired distribution of the doping profile along the cell surface is extremely simplified when laser processing is used leading to selective emitters. Local diffusions have been proposed [3-4] and even more complicated structures can be defined by guiding the laser radiation into a chemical liquid jet [5].

In the last years, our group has been working on c-Si surface passivation by amorphous silicon carbide (a-SiC_x:H) deposited by PECVD with excellent results [6-8]. Particularly, a stack of these films have been proposed as n^+ emitter passivation and anti-reflecting layer [9]. The addition of phosphorus to these films is easily achieved by introducing phosphine (PH₃) into the precursor gases leading to a-SiC_x:H (n) films.

We propose the idea of local phosphorus diffusions by means of laser processing using a-SiC_x:H (n) films as the doping source with the final goal of being applied into a c-Si solar cell. In this work, we demonstrate the viability of the laser processed local phosphorus diffusions by means of two laser wavelengths 1064 nm and 532 nm. Particularly, we focus on the morphological and electrical performances of these emitters.

On the other hand, in another contribution also presented in this conference [10], we study the problems related to the presence of a discontinuous n^+ emitter. It is well known that dielectric films such a-SiC_x:H or a-SiN_x:H have a high positive fixed charge density that attracts electrons to the surface creating an inversion layer. In that contribution, we propose novel solar cell structures to create an inversion layer in between n^+ diffusions less dependent on the fixed charge density of the dielectric film.

2. EXPERIMENTAL

Two different laser systems were employed for the laser patterning. The first one is a Nd:YAG 15 nanosecond pulsed laser emitting at 532 nm (Spectra physics Model Navigator X15SC-532Q) at a frequency rate of 15 to 100 KHz. The number of applied laser pulses was controlled by means of an electro-mechanical shutter and the pulse energy was varied changing the current of the LED diode which is pumping the laser medium from 18 A to 20 A. Target holder was placed on motorized translation axes.

The 1064 nm laser used in this work is a Q-switched Nd:YAG laser (StarMark SMP 100II Rofin-Baasel) that emits at 1064 nm in TEM₀₀ mode with a pulse duration fixed at 100 nanosecond. The energy of the laser beam can be adjusted by varying the intensity of the continuous lamp that pumps the Nd:YAG crystal. The laser beam is guided by rotating mirrors before the focusing lens (focal length 254 mm) that allow to process samples up to 8 inches. In this work, the laser is conducted in pulsed mode and we varied the control current of the lamp from 16 A to 18 A, and the number of shots per spot from 1 to 10 pulses, maintaining the pulse repetition rate to a fixed value of 4 kHz.

In order to study the morphology of the laser patterns, Scanning Electron Microscopy (SEM, HITACHI S-3000N and ZEISS NEON 40) and optical profilometry with Confocal Scanning Laser Microscope (Leica ICM 1000) and White Light Interferometer (Wyko NT-110 Veeco Instruments) analyses were employed. In addition, the profiles of phosphorous concentration in the crystalline silicon were determined by Secondary Ion Mass Spectroscopy (SIMS).

The phosphorus doped $a\text{-SiC}_x\text{H}$ film was deposited by PECVD (PlasmaLab DP 80) and the technological parameters of its deposition are described elsewhere [9]. The thickness of the deposited film was about 100 nm.

To evaluate the electrical performance of the emitters, we prepared matrixes of 100 to 289 point diffusions separated 300 μm for the ones processed with the 532 nm laser and 250 μm for the infra-red one. The p-type ($\rho = 1\text{-}3 \Omega \text{ cm}$) substrate was contacted with evaporated aluminum at the back and the n^+ emitters with squares of 5x5 mm of e-gun evaporated Ti/Pd/Ag that completely covered the point matrix. In figure 1 we show a schematic structure of these samples. The dark current density–voltage ($J\text{-}V$) characteristics were measured with impedance analyzer HP4142B.

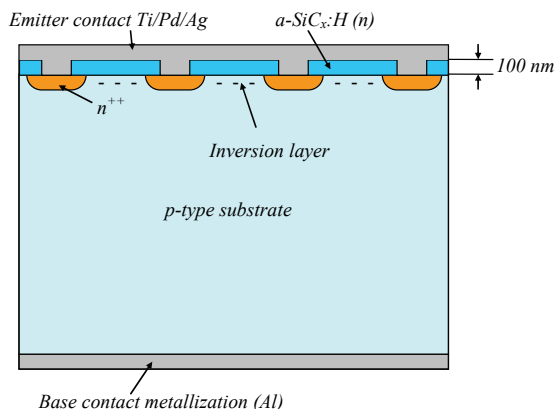


Figure 1. Schematic diagram of samples prepared for J-V measurements.

3. MORPHOLOGICAL RESULTS

3.1 SIMS measurement

Firstly, in order to obtain an experimental confirmation of the phosphorus diffusion, we measured the phosphorus profile by SIMS in two samples processed with the 532 nm laser. The preparation of a suitable sample for the SIMS measurement consisted in a scanning laser processing upon a $1 \times 0.8 \text{ mm}^2$ area to generate 25% overlapped craters of 50 μm diameter. The laser parameters used for that purpose were the following: 20 KHz frequency, two pulses per laser point and two different pulse energies: 50 μJ and 110 μJ . Additionally, as a reference we also measured on a region with no laser processing labeled as “No laser treatment”, i.e. c-Si covered with the phosphorus doped $a\text{-SiC}_x\text{H}$ film. The results are shown in figure 2. For the sample without laser treatment, the phosphorus is concentrated on a thin region close to the surface that corresponds to the $a\text{-SiC}_x\text{H}(n)$ film and no diffusion into the c-Si is observed. For both laser-processed samples, this surface accumulation of atoms is lost and replaced by a soft phosphorus profile that goes deep into the c-Si. In this

case, the signal in counts/s can be directly compared between both samples since the matrix where the atoms are embedded is the same. With the low energy pulses a high phosphorus concentration is obtained that slightly decreases deep in the c-Si. On the other hand, with high energy pulses the phosphorus concentration is decreased by about an order of magnitude at the surface, probably due to excessive energy pulse that evaporates the material. From these results, we can conclude that the phosphorus is diffused and that the pulse energy can control the phosphorus profile.

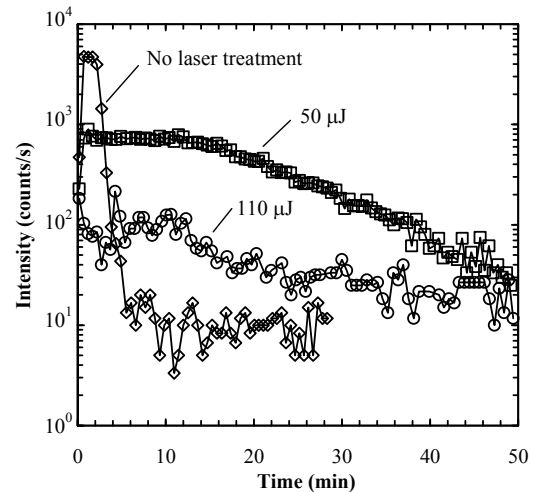


Figure 2. Phosphorus profiles measured by SIMS for two samples processed with the 532 nm laser at two pulse energies of 50 μJ and 110 μJ . Additionally, a non-processed sample is also shown for comparison.

3.2 SEM and optical profilometry analysis

In figure 3 we show SEM pictures and optical profilometry of 1064 nm laser processed samples. In this case, we varied the pulse energy ranging from 250 μJ to 450 μJ . We can see that when pulse energy increases the diameter of the affected region also increases, ranging from 26 μm to 82 μm . With the lowest pulse energy the c-Si is not melted and the $a\text{-SiC}_x\text{H}$ film is ablated as it is deduced from the fact that the depth of the hole corresponds to the film thickness. The other three measured profiles show a cone at the center of the spot that increases its height with energy and finally collapses for the highest pulse energy. This is the typical behavior of a melted surface that is ejected and solidified again at different stages, similar to a water droplet.

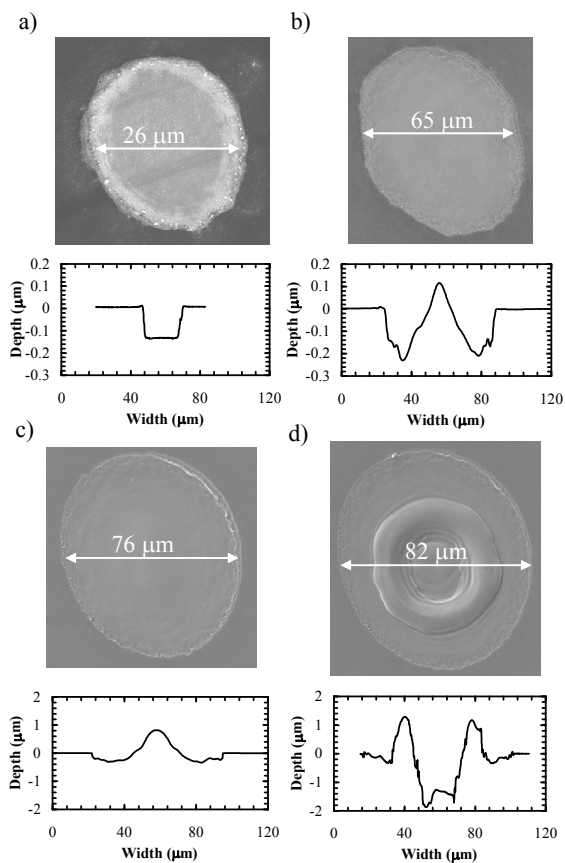


Figure 3. SEM pictures and optical profilometry of 1064nm laser processed points at different pulse energy: a) 250 μJ , b) 320 μJ , c) 380 μJ and d) 450 μJ .

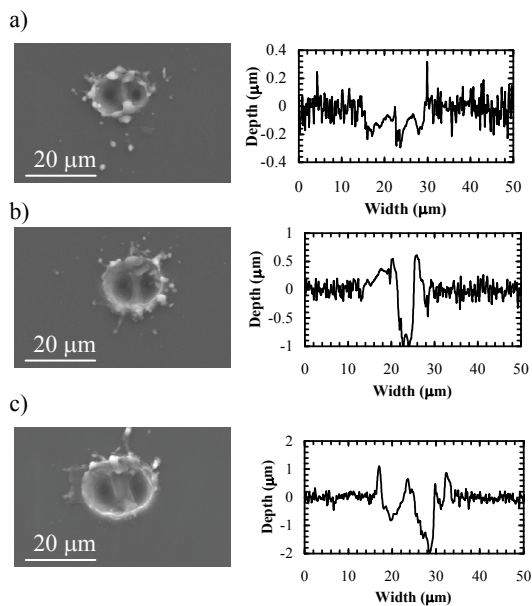


Figure 4. SEM pictures and optical profilometry of 532nm laser processed points at different pulse energy: a) 3.1 μJ , b) 5 μJ and c) 8 μJ .

The results related to the 532 nm laser are presented in figure 4 where the pulse energy was varied from 3.1 μJ to 8 μJ keeping constant the number of pulses to five. In

all the samples, two clear holes can be observed indicating that the laser beam is not perfectly Gaussian. In this case, the diameter of the affected area is almost constant to about 20 μm , smaller than the ones obtained with the 1064 nm laser where the pulse energy is nearly two orders of magnitude high. The presence of material melting in the border of the crater and droplets evidences the thermal character of the nanosecond laser ablation process that leads to the formation of a liquid layer. The observed morphologies are consistent with a rapid expulsion of droplets cooling and solidifying quickly.

4. ELECTRICAL RESULTS

Regarding the 1064 nm laser, firstly we investigated the dependence of J-V curves on the energy pulse. The results are shown in figure 5. As it can be observed, an optimum J-V curve is obtained for a pulse energy of 320 μJ . Lower pulse energy leads to a non-ideal diode and a high contact resistance between the metal and the diffused n^+ regions. On the other hand, higher pulse energy reveals an exponential trend similar than the optimum one but with a higher saturation current density (J_0). Additionally, the contact is also worse compared to the optimum. Next, for the optimum energy pulse found, we investigated the effect of the number of pulses on the J-V curve resulting in the plot shown in figure 6. The trend is identical to the one obtained with the energy: more pulses increase the J_0 of the diode and worsen the contact resistance.

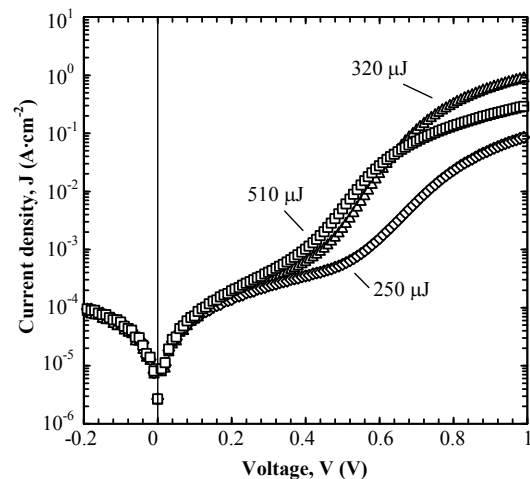


Figure 5. J-V curves of diodes fabricated with 1064 nm laser at different pulse energies with five pulses per point.

For the 532 nm laser, we also studied the dependence of the J-V curves on the energy pulse whose results are shown in figure 7. The number of pulses per diffused point was five. In this case, the optimum observed corresponds to the minimum pulse energy available in the laser. As the pulse energy is increased the contact resistance increases and the almost ideal exponential behavior is progressively lost. It seems that the n^+ -p junction is replaced in some way by a diode with a much lower energy barrier resulting in a dramatic increase of the current for low voltages.

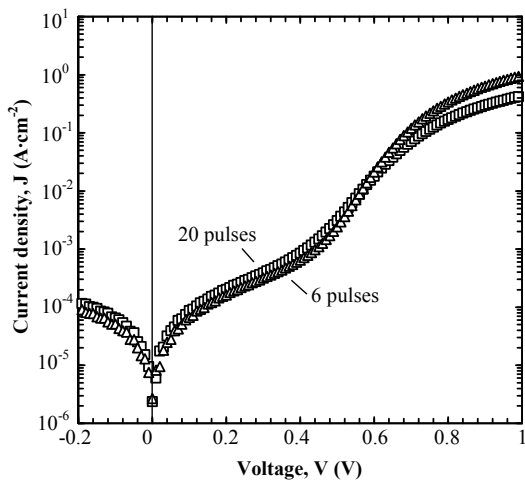


Figure 6. J-V curves of diodes fabricated with 1064 nm laser at an energy pulse of 3.2 μJ with 6 and 20 pulses per diffusion point.

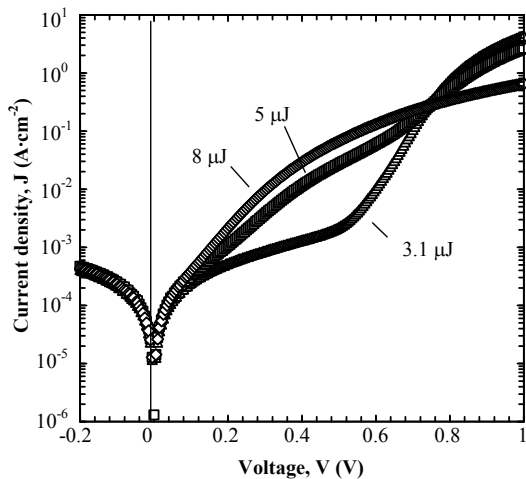


Figure 7. J-V curves of diodes fabricated with 532 nm laser at different pulse energies with five pulses per point.

All these results could be interpreted as following: for both lasers there is an optimum pulse energy that provides a good phosphorus diffusion profile, low c-Si damage and a surface phosphorus concentration high enough to create a reasonably good ohmic contact between the n^+ regions and the titanium. For lower energies, the phosphorus is not properly diffused or activated leading to non-ideal J-V curves. Additionally, due to the lack of active doping atoms the contact resistance is also high. For higher energies than the optimum, some differences can be observed depending on the laser wavelength. For the 1064 nm laser, an increase in the J_0 and the contact resistance is observed indicating that the phosphorus diffuses deeper into the c-Si. Then, a more recombining n^+ region is created and, due to the finite dose of phosphorus atoms located at the a-SiC_x:H(n) film, the deeper the diffusion the lower the surface phosphorus concentration. This would explain the worse contact resistance. Regarding the 532 nm laser, this effect could be also observed in the comparison of the 5 μJ sample to the 3.1 μJ one. However, for high energy pulses the strong increase of current for low

voltages could be interpreted as a Schottky diode between the titanium and the p-type substrate. The 532 nm laser has a less thermal interaction and do not seems to help phosphorus atoms to diffuse but seems to evaporate them. In that case, we could have a behavior closer to a-SiC_x:H(n) ablation. Then, the metal would be evaporated directly on the p-type substrate where it is well-known that the titanium would create a Schottky barrier. Additionally, the strong increase in the contact resistance observed for the highest pulse energy also indicates a low phosphorus concentration.

Best results for both lasers are plotted in figure 8 where the measured current has been divided by the matrix area allowing a direct comparison. It can be observed that the 532 nm laser results in a slightly better J-V dependence with lower J_0 and contact resistance. We think that the improvement in J_0 with the 532 nm laser could be mainly related to the difference in the diameter of the points explained in the previous subsection. Apart from differences in the phosphorus diffusion that must be addressed in further investigations, the different point size could also play an important role since the diameter is reduced from about 60 μm to about 20 μm . This means a factor of 9 in area that directly impacts on the J_0 . On the other hand, it seems that the less thermal and, hence, more superficial interaction of the 532 nm laser could help to maintain a high phosphorus surface concentration resulting in an excellent contact resistance.

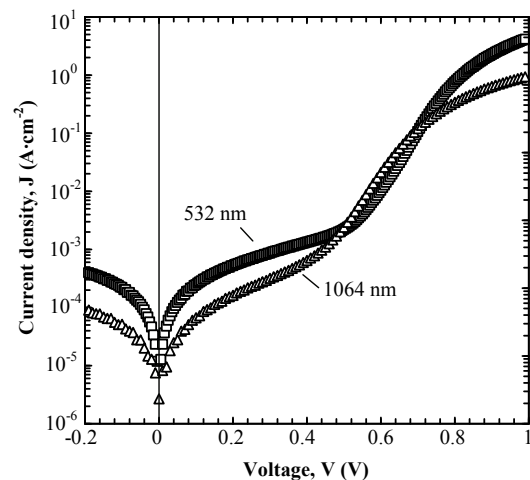


Figure 8. Best J-V curves of diodes fabricated with 1064 nm and 532 nm lasers.

Finally, finished solar cells are planned to be fabricated based on these best results. The planned structure is shown in figure 9. Notice that the n^+ -p junction are placed at the back of the solar cell since a fully area metallization is needed. Additionally, an aluminum oxide (Al_2O_3) film is deposited onto the front face of the cell for surface passivation. Recently, these films have revealed excellent surface passivating properties based on a high negative fixed charge density that accumulates holes at the interface [11]. Extrapolating the dark J-V curves to $1 \times 1 \text{ cm}^2$ devices and assuming that the main recombination will be located at the laser processed emitter, we expect to reach V_{oc} in the range of

620 mV and 640 mV for the 1064 nm laser and the 532 nm laser, respectively. The obtained results with such devices will be published elsewhere.

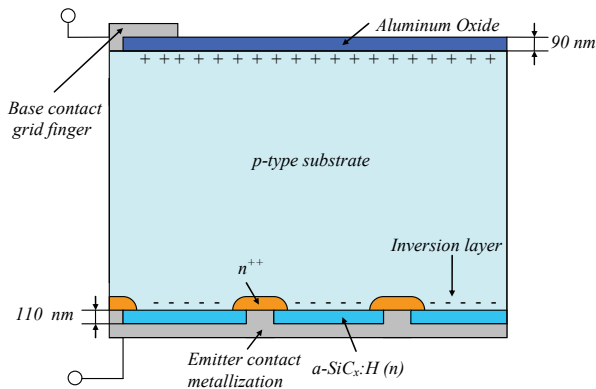


Figure 9. Solar cell structure planned to be fabricated based on the best results for the n^+ formation with 1064 nm and 532 nm lasers.

5. CONCLUSIONS

The viability of laser processed phosphorus diffusions using $a\text{-SiC}_x\text{:H}(n)$ as doping source is demonstrated with both laser wavelengths 1064 nm and 532 nm. This laser treatment allows us to obtain a diffused emitter in a very simple process with low thermal affectation. Morphological analysis shows that, in the irradiation conditions of this work, the 1064 nm laser creates 30-80 μm diameter craters whereas the green one shows smaller affected regions of about 20 μm diameter. The electrical characterization helps us to determine the optimum parameters for every laser revealing that a fine tune of the pulse energy is crucial. Comparing the best results of both lasers, the 532 nm laser sample is slightly better with better contact resistance and lower saturation current density. The expected V_{oc} for solar cells based on this emitter is in the range of 640 mV.

ACKNOWLEDGMENTS

This work has been supported by the Spanish Government through the projects TEC-2008-02520/TEC and PSE-MICROSIL08 (PS-120000-2006-6).

REFERENCES

- [1] A. Esturo-Breton, M. Ametowobla, C. Carlsson, J. Köhler, J. Werner, Proceedings of 21st European Photovoltaic Solar Energy Conference, 2006; 1247.
- [2] K. Horiuchi, Y. Nishihara, A. Ogane, Y. Takahashi, A. Kitiyanan, Y. Uraoka, T. Fuyuki, Proceedings of 22nd European Photovoltaic Solar Energy Conference, 2007; 1423.
- [3] S.W. Glunz, A. Grohe, M. Hermle, E. Schneiderlöchner, J. Dicker, R. Preu, H. Mäkel, D. Macdonald, A. Cuevas, Proceedings of 3rd World Conference Photovoltaic Energy Conversion, 2003; 1332.
- [4] B.S. Tjahjono, J.H. Guo, Z. Hameiri, L. Mai, A. Sugianto, S. Wang, S.R. Wenham, Proceedings of 22nd

European Photovoltaic Solar Energy Conference, 2007; 966.

[5] S. Hopman, A. Fell, K. Mayer, M. Aleman, M. Mesec, R. Müller, D. Kray, G.P. Willeke, Proceedings of 22nd European Photovoltaic Solar Energy Conference, 2007; 1257.

[6] I. Martín, M. Vetter, A. Orpella, J. Puigdollers, A. Cuevas, and R. Alcubilla, Appl. Phys. Lett. 79, 2199 (2001).

[7] I. Martín, M. Vetter, A. Orpella, C. Voz, J. Puigdollers, and R. Alcubilla, Appl. Phys. Lett. 81, 4461 (2002).

[8] R. Ferre, A. Orpella, D. Muñoz, I. Martín, F. Recart, C. Voz, J. Puigdollers, P. Roca i Cabarrocas and R. Alcubilla, Prog. Photovolt.: Res. Appl. 16, 123 (2008).

[9] R. Ferre, I. Martín, P. Ortega, M. Vetter, I. Torres, R. Alcubilla, J. Appl. Phys. 100, 073703 (2006).

[10] I. Martín, R. Löyblom, R. Alcubilla, "High-efficiency solar cells based on inversion layer emitters", presented at this conference.

[11] B. Hoex, J.J.H. Gielis, M.C.M. van de Sanden, W.M.M. Kessels, J. Appl. Phys. 104, 113703 (2008).